

Eddy viscosity and hyperviscosity in spectral simulations of 2D drift wave turbulence

S. A. Smith

*Department of Applied and Computational Mathematics, Princeton University,
Princeton, New Jersey 08544*

G. W. Hammett

Princeton Plasma Physics Laboratory, P.O. Box 451, Princeton, New Jersey 08543

(Received 5 August 1996; accepted 17 December 1996)

A wavenumber dependent eddy viscosity is calculated for a simple two-dimensional drift wave model from direct numerical simulations for a wide range of parameters and cutoff wavenumber. The damping rate given by this eddy viscosity is well modeled by a hyperviscosity, where the power and magnitude are parameterized as functions of the shear in the resolved advecting velocity. Tests in simulations with low resolution find that the use of this parameterized hyperviscosity yields somewhat better results than the use of hyperviscosity with fixed power and is significantly better than the use of no extra damping term or a Smagorinsky type eddy viscosity. This parameterized hyperviscosity is very useful computationally, since reducing resolution requirements by even a factor of 2 reduces the computational requirements by a factor of 8 in two dimensions, or 16 in three dimensions. © 1997 American Institute of Physics. [S1070-664X(97)00204-8]

I. INTRODUCTION

Models for the subgrid scale dissipation in numerical simulations of turbulence have long been necessary in the study of atmospheric and oceanographic turbulence, where the direct numerical simulation of the full range of scales is infeasible.¹ “Large Eddy Simulations” (LES) evolve the largest scales of a problem and model the average interaction with the unresolved small scales through dissipative terms called eddy viscosity. Our goal is to apply these techniques to simulations of drift wave turbulence in tokamaks. This preliminary study tests some basic dissipative terms in a simple two-dimensional (2D) drift wave model. By restricting the problem to two dimensions, a large number of simulations can be performed with sufficient time histories for the statistics necessary to compute the eddy viscosity. The resulting parameterization of the eddy viscosity has been successfully applied to fully three-dimensional (3D) simulations of drift wave turbulence which will be reported in a future paper.

When it is computationally impossible to resolve the dissipation scales in homogeneous isotropic turbulence, the standard tool used in numerical simulations is hyperviscosity, a damping rate of the form $M|\mathbf{k}|^p$, where the power p is larger than 2 which gives ordinary viscosity. Hyperviscosity introduces an artificial dissipation range into the problem, that is narrower than the usual dissipation range and therefore requires less resolution. The choice of power and magnitude is somewhat arbitrary. Numerical studies of 2D Navier-Stokes turbulence have found that a moderately high power ($p=8$ or $p=16$) allows the hyperviscosity to effectively remove energy from small scales with a minimum of unphysical dissipation at the large scales.² While the dissipation range introduced by hyperviscosity acts as a model for the true dissipation range, the damping provided by hyperviscosity has not been systematically compared with the nonlinear transfer rates to unresolved scales.

Eddy viscosities attempt to model the sink of energy at small scales by introducing dissipation into the resolved scales. The Smagorinsky nonlinear viscosity,³ for example, is a simple model with a long history of applications in fluid turbulence. The damping given by the Smagorinsky viscosity is proportional to $|\mathbf{k}|^2$, which is rigorously correct only in the limit where the separation of scales between resolved and unresolved modes is asymptotically large. When there is significant transfer of energy that is local in k -space, as in Navier-Stokes turbulence, the contribution to the eddy viscosity from local transfer to unresolved modes near the cutoff is poorly represented by a k^2 damping rate.⁴ A theoretical eddy viscosity has been tested for the inverse cascade range in large eddy simulations of 2D Navier-Stokes turbulence.⁵

The ideas of hyperviscosity and eddy viscosity are combined here to create a nonlinear filter for use in simulations of drift wave turbulence. Since theoretical predictions of the nonlinear transfer do not exist for comprehensive models of drift wave turbulence (or even for the simple model considered here), the hyperviscosity model is chosen by comparison with direct numerical simulations. The eddy viscosity is calculated for a given set of parameters and resolution from a higher resolution simulation by calculating the transfer from modes that are contained in the low resolution simulation to all other modes. We calculate the eddy viscosity in this fashion for a wide range of parameters and various resolutions. We then fit this damping rate by adjusting the hyperviscosity power and magnitude. The power p and magnitude M were then parameterized as functions of the resolved modes based on insights from Kraichnan's eddy viscosity for the 2D enstrophy range.

The resulting parameterized hyperviscosity has several advantages over traditional approaches. The choice of power and magnitude are calculated from functions of the resolved scales, eliminating what are arguably free parameters in the

standard application of hyperviscosity. The damping rate comes closer to modeling the actual eddy damping rate than eddy viscosities like Smagorinsky's which have damping rates proportional to k^2 . For problems of interest, the actual eddy damping rate has not been predicted theoretically and can only be calculated from high resolution simulations. This method is straightforward to implement in spectral simulations of homogeneous turbulence, where k -dependent damping rates are trivial to incorporate.

The parameterization is based on the general physical processes of nonlinear advection and 2D enstrophy cascade. We therefore expect this model to be useful for more general drift wave calculations which resolve the main energy injection scales, and are using this hyperviscosity only to reduce the resolution needed for modes at scales smaller than the injection scales. This model may also be useful for passive scalar advection problems. Situations with inverse cascade and significant energy production at unresolved scales, such as may be found in magnetohydrodynamic turbulence or 2D Navier-Stokes turbulence, result in negative eddy viscosities and are therefore clearly beyond the scope of this model, but have been studied with other models.⁵

II. MODEL EQUATIONS

The model equation for this study was chosen to be as simple as possible while retaining the basic physics relevant to subgrid turbulence processes in fluid simulations of drift wave turbulence. Saturation in toroidal gyrofluid turbulence simulations⁶ involves a balance between the source of fluctuations in linearly unstable modes and the dissipation in modes that are stabilized by terms that model Landau damping.⁷ Fluctuation energy is transferred from unstable to stable modes through the advection nonlinearity. A useful 2D model will at the least contain the $\mathbf{E} \times \mathbf{B}$ drift advection nonlinearity, a linear instability, and dissipation to model Landau damping, which is primarily a function of the parallel wavelength and should therefore be present at long perpendicular wavelengths. Though the system we will study in this paper includes models of these three essential effects, it is a relatively simple one-field 2D equation which results from major simplifications and approximations. For example, it is missing the bad curvature and ion temperature dynamics which are important instability mechanisms in the core region of many tokamaks. As a 2D model, it is missing a special constraint on the adiabatic electron response which enhances the role of the $k_y = k_z = 0$ component of the electrostatic potential,⁸ leading to turbulence-generated sheared flows which are important in toroidal simulations.^{9,6,10,11} Nevertheless, the system used in this study is a useful paradigm for studying certain effects important in plasma turbulence where the $\mathbf{E} \times \mathbf{B}$ nonlinearity is important, and some of the lessons learned in this simple model can then be applied in more complicated three-dimensional multi-field simulations.

There is a significant literature on two-dimensional models for drift wave turbulence. The prototypical model of Hasegawa and Mima¹² captures the basic physics of the $\mathbf{E} \times \mathbf{B}$ nonlinearity in a one-field 2D equation, but contains no linear drive to produce fluctuations. So-called “ $i\delta$ ” equa-

tions,^{13,14} introduce linear drive through a simple model for the non-adiabatic part of the electron response. The model equation derived here is a simplified “ $i\delta$ ” model, with an additional term added to model Landau damping at long wavelengths.

There are a number of derivations in the literature of this model starting from standard fluid equations. Here we sketch the derivation from a gyrokinetic/gyrofluid perspective. The starting point is just a conservation equation for the ion guiding center density n_{gc}

$$\frac{\partial n_{gc}}{\partial t} + \nabla \cdot [n_{gc}(\mathbf{v}_E + u_{\parallel} \hat{\mathbf{z}})] = 0, \quad (1)$$

where

$$\mathbf{v}_E = (c/B) \hat{\mathbf{z}} \times \nabla \phi \quad (2)$$

is the $\mathbf{E} \times \mathbf{B}$ drift velocity, ϕ is the potential, and u_{\parallel} is the parallel ion flow. Most of the ion FLR effects are ignored (via the assumption $T_i \ll T_e$) while the ion polarization effects are retained by including the ion polarization density in addition to the guiding center density in determining the actual ion density

$$n_i = n_{gc} + n_0 \frac{\rho_s^2 e}{T_e} \nabla_{\perp}^2 \phi, \quad (3)$$

where $\rho_s = c_s / \Omega_{ci}$ is the gyroradius using the ion gyrofrequency, $\Omega_{ci} = eB/m_i c$, and the sound speed, $c_s = \sqrt{T_e/m_i}$. (This approach is the standard method used in the gyrokinetic Poisson equation.¹⁵⁻¹⁷) For the ion parallel flow velocity, we will use a “1-moment” model of Landau damping,¹⁸

$$n_0 \frac{d}{dz} u_{\parallel} \approx C_1 v_t |k_{\parallel}| (n + \phi) \approx C_2 v_t |k_{\parallel}| n, \quad (4)$$

where C_1 and C_2 are constants of order unity. Making use of the standard two-scale approximations (see Ref. 18 for some of our notation) to expand n_{gc} in Eq. (1) via

$$n_{gc} = n_0 \left(1 + \frac{x - x_0}{L_n} \right) + \tilde{n}_i \quad (5)$$

into a long scale equilibrium part with density gradient scale length, L_n , and a short scale fluctuating component \tilde{n}_i , leads to

$$\begin{aligned} \frac{\partial \tilde{n}_i}{\partial t} + \mathbf{v}_E \cdot \nabla \tilde{n}_i + \frac{n_0 e c_s \rho_s}{T_e} \frac{\partial \phi}{L_n \partial y} \\ = -\alpha \frac{c_s}{L_n} \tilde{n}_i + \mu \frac{c_s \rho_s^2}{L_n} \nabla_{\perp}^2 \tilde{n}_i, \end{aligned} \quad (6)$$

The density gradient in the long scale equilibrium introduces the diamagnetic drift term containing the derivative of the potential. The collisional viscosity, μ , is expected to be small, but is included to provide a sink for fluctuation energy at high k . The other dissipative term, $\alpha \tilde{n}_i$, introduces damping at long wavelengths and is intended as a simple model for the Landau damping caused by a small but finite k_{\parallel} [$\sim (qR)^{-1}$ in a tokamak]. Three-dimensional simulations of drift wave turbulence have found that the bulk of the dissipation comes from Landau damping,⁶ so it is necessary to

include a model for this process in 2D simulations where k_{\parallel} has been ignored. A simple fluid model for Landau damping would set the damping rate, $\alpha c_s/L_n$, proportional to $|k_{\parallel}|v_t$.⁷

To close the model system, we must relate the fluctuation density to the potential. The real space ion density, δn_i , is just the sum of the guiding space density, \tilde{n}_i , and the ion polarization density, $\rho_s^2 \nabla_{\perp}^2 e \phi / T_e$. As a crude model for the electron response that will provide linear drive we set $\delta n_e = (1 - \delta_0 \rho_s \partial / \partial y) e \phi / T_e$. Quasineutrality therefore gives us

$$\tilde{n}_i = \frac{n_0 e}{T_e} \left(1 - \rho_s^2 \nabla_{\perp}^2 - \delta_0 \rho_s \frac{\partial}{\partial y} \right) \phi. \quad (7)$$

Using normalized variables,

$$\tau = \frac{c_s}{L_n} t, \quad x' = x \rho_s, \quad y' = y \rho_s, \quad \psi = \frac{L_n}{\rho_s} \frac{e}{T_e} \phi, \quad (8)$$

and then dropping the primes we obtain the evolution equation,

$$\left(\frac{\partial}{\partial \tau} + \alpha - \mu \nabla_{\perp}^2 \right) \left[1 - \nabla_{\perp}^2 - \delta_0 \frac{\partial}{\partial y} \right] \psi + \hat{\mathbf{z}} \times \nabla \psi \cdot \nabla \left[-\nabla_{\perp}^2 - \delta_0 \frac{\partial}{\partial y} \right] \psi + \frac{\partial \psi}{\partial y} = 0. \quad (9)$$

Expressing the potential as a sum of Fourier modes, $\psi = \sum_{\mathbf{k}} \exp(i\mathbf{k} \cdot \mathbf{x}) \psi_{\mathbf{k}}$, gives the mode coupling equation,

$$\left(\frac{\partial}{\partial \tau} + i\omega_{\mathbf{k}} - \gamma_{\mathbf{k}} - \gamma_{\mathbf{k}}^d \right) \psi_{\mathbf{k}} = N_{\mathbf{k}}, \quad (10)$$

where the nonlinear term is defined as,

$$N_{\mathbf{k}} = \sum_{\mathbf{k}'} \frac{\hat{\mathbf{z}} \times \mathbf{k}' \cdot \mathbf{k} [|\mathbf{k} - \mathbf{k}'|^2 - i\delta_0(k_y - k'_y)]}{1 + |\mathbf{k}|^2 - i\delta_0 k_y} \psi_{\mathbf{k}'} \psi_{\mathbf{k} - \mathbf{k}'}, \quad (11)$$

and the linear frequency and growth rate are given by,

$$\omega_{\mathbf{k}} = \frac{k_y (1 + |\mathbf{k}|^2)}{(1 + |\mathbf{k}|^2)^2 + \delta_0^2 k_y^2}, \quad (12)$$

$$\gamma_{\mathbf{k}} = \frac{\delta_0 k_y^2}{(1 + |\mathbf{k}|^2)^2 + \delta_0^2 k_y^2} - \alpha - \mu |\mathbf{k}|^2. \quad (13)$$

We have introduced an additional growth rate, $\gamma_{\mathbf{k}}^d$, for the dissipation model which can be defined to be the regular hyperviscosity given by Eq. (33) or the parameterized hyperviscosity given by Eq. (36) or set to zero. [The Smagorinsky eddy viscosity of Eq. (22) does not have the form of a simple damping rate in k -space.] The linear physics of this model agrees with a model for dissipative trapped electron drift waves derived by Liang *et al.*¹⁴ to first order in δ_0 (D_0 in their notation) and second order in $k\rho_s$. Setting $\alpha = 0$, $\mu = 0$, and $\delta_0 = 0$, gives the equation of Hasegawa and Mima.¹²

The model equation used here was chosen for simplicity and only contains the gross features of drift wave turbulence. To be of practical use, in fact, our results concerning eddy viscosity should not depend on the precise nature of Eq. (9),

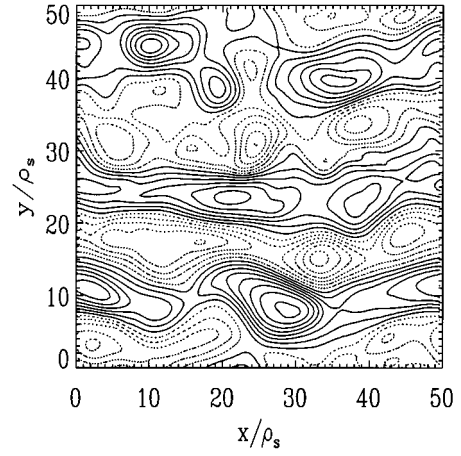


FIG. 1. Contours of potential for saturated turbulence at one instant.

since we are interested in applications to more sophisticated models of drift wave turbulence. The toroidal gyro-fluid equations,^{6,19} which evolve multiple fields and contain significantly more complicated (hence more accurate) linear physics, share the same basic nonlinear advection term contained in this model. Hence the eddy viscosity calculated in this study is parameterized as a function of the advecting velocity without reference to the linear physics.

III. PHYSICS OF THE SATURATED STATE

Before considering the effects of subgridscale effects, we examine the results of simulating the model, Eq. (9), for a typical set of parameters. Simulations were performed with periodic boundary conditions using the standard dealiased pseudospectral approach. A hyperviscous damping term of the form discussed in the next section was used for the results considered here. Initially we consider a box of size $50\rho_s \times 50\rho_s$, using a 128×128 grid in real space, for parameters $\delta_0 = 0.35$, $\alpha = 0.035$, and $\mu = 0.0001$, with a hyperviscosity defined by Eq. (33) with power $p = 16$ and coefficient set to the average rate of shear, $v_h = S(t)$. [See Eq. (34).] This choice of δ_0 gives growth rates large enough that the saturated state is in the strong turbulence regime. The instantaneous potential late in the simulation is shown in Fig. 1.

One useful macroscopic parameter that can be expressed in this model is the volume averaged particle flux,

$$\begin{aligned} \Gamma &= \frac{1}{A} \int \hat{\mathbf{x}} \cdot \mathbf{v}_E \tilde{n}_i d\mathbf{x} \\ &= \delta_0 \left(\frac{cT_e}{eB} \frac{\rho_s}{L_n} \right) \frac{n_0}{L_n} \sum_{\mathbf{k}} k_y^2 |\psi_{\mathbf{k}}|^2. \end{aligned} \quad (14)$$

The gyro-Bohm scaling of the flux is the natural scaling for this system, since the use of periodic boundary conditions and a constant background gradient prevents the system scale from directly entering the analysis. (The system scale could in principle enter through the size of the simulation domain $L_x \times L_y$, implying a Bohm scaling. The fact that such ‘‘flux-tube’’ simulations saturate,^{20,21} and that the saturation amplitude is independent of the size of the simulation

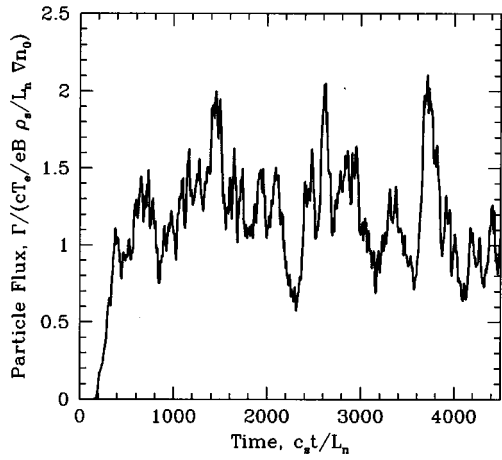


FIG. 2. Particle flux from simulation of the model equation in a periodic box ($50\rho_s \times 50\rho_s$) in the strong turbulence regime, $\delta_0=0.35$, $\alpha=0.035$, $\mu=0.0001$.

domain indicates that a gyro-Bohm scaling regime exists for sufficiently small ρ_s/L_n . The time history of the flux for our initial set of parameters is shown in Fig. 2.

Since observable physical quantities such as the particle flux and mean square density fluctuations can be expressed as quadratic functions of the potential, one is led to study the evolution and saturation of the squared magnitude of the modes. There is only one quadratic quantity that is conserved by the nonlinear term of our model, Eq. (9), corresponding to the fact that the volume integrated square density, $\int \tilde{n}_i(\mathbf{x})^2 d\mathbf{x}$, is conserved by divergence free advection. We will denote this conserved quantity, Ω , and define a normalized modal contribution to the conserved quantity,

$$\Omega_{\mathbf{k}} = \frac{1}{2} [(1 + |\mathbf{k}|^2) + \delta_0^2 k_y^2] |\psi_{\mathbf{k}}|^2. \quad (15)$$

Figure 3 displays the saturated spectrum for the initial set of parameters, where the standard two-dimensional spectral density is defined by, $\Omega(k) = 2\pi k \langle \Omega_{\mathbf{k}} \rangle$, where the average is

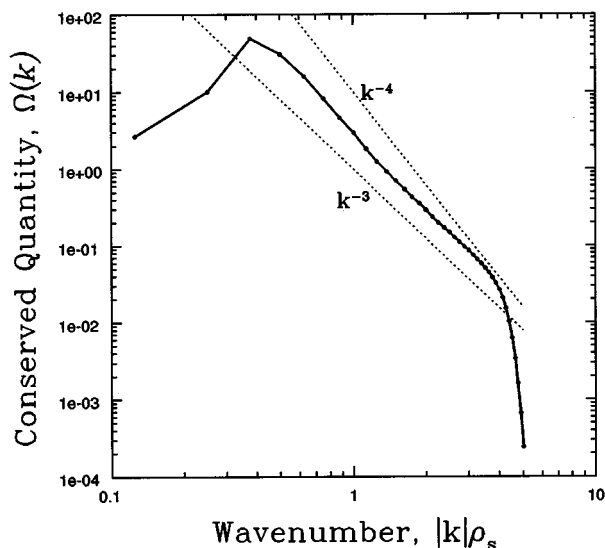


FIG. 3. Time averaged spectrum of density fluctuations for the simulation of Fig. 2.

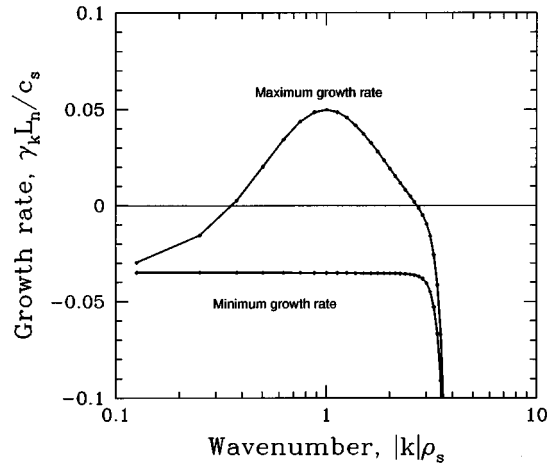


FIG. 4. Growth rates for the simulation of Fig. 2. A k^{16} hyperviscosity damping term has been used to improve the resolution of the inertial range.

taken over the band of \mathbf{k} 's at radius k . (The growth rates for this simulation are displayed in Fig. 4.) Attempting to infer an inertial range power law scaling from this spectrum would give $\Omega(k) \sim k^p$ with $-4 \lesssim p \lesssim -3$ which is very different from the 2D Navier-Stokes high k inertial range where enstrophy scales as k^{-1} .^{22,23} In fact, simulations of 2D Navier-Stokes turbulence have typically observed inertial ranges significantly steeper than theoretically predicted. The k^{-1} enstrophy range is an asymptotic limit that can only be observed when the dissipation scales are separated from the forcing scales by at least two orders of magnitude.²⁴ The separation of scales required to observe inertial range scaling is particularly large in 2D turbulence, where the enstrophy transfer is very nonlocal. Such a scenario is highly unlikely for plasma turbulence problems where significantly damped modes exist at wavenumbers very close to the unstable modes driving the turbulence. Therefore, one should not expect to find universal exponents in drift wave simulations.

The evolution equation for this quadratic invariant is just,

$$\left(\frac{\partial}{\partial \tau} - 2\gamma_{\mathbf{k}} \right) \Omega_{\mathbf{k}} = T_{\mathbf{k}}, \quad (16)$$

where the nonlinear transfer, $T_{\mathbf{k}}$, is given by,

$$T_{\mathbf{k}} = [(1 + |\mathbf{k}|^2) + \delta_0^2 k_y^2] (\psi_{\mathbf{k}} N_{\mathbf{k}}^* + \psi_{\mathbf{k}}^* N_{\mathbf{k}}). \quad (17)$$

In steady state, the nonlinear transfer balances the production and dissipation of fluctuations due to linear growth or damping. (See Fig. 5 for typical example of the linear production.) For two-dimensional equations of this form, with only one quadratic invariant, it has been noted that arguments from statistical mechanics imply transfer to small scales,²⁵ in contrast to the dual cascade picture from 2D Navier-Stokes turbulence. With moderate dissipation due to Landau damping at all scales, there is no clearly defined inertial range or cascade. The production of the conserved quantity for a typical run is plotted in Fig. 5. Note that the dominant source and the major sink for fluctuation energy both lie near the peak of the spectrum. The major transfer in k -space of fluctuation energy is in fact not a cascade, and

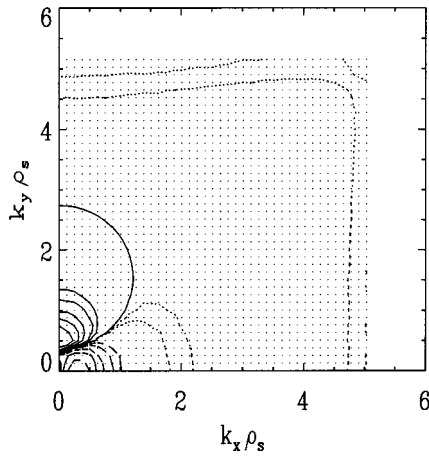


FIG. 5. Time averaged production and dissipation of density fluctuations for the simulation of Fig. 2 (contours of $\langle \gamma_{\mathbf{k}} \Omega_{\mathbf{k}} \rangle$). Each point is a resolved mode. Solid lines are contours of the production region at 0, 1, 2, 5, 10, and 20 (dimensionless units). Dashed lines are contours of the dissipation region at $-1, -2, -5, -10$, and -20 . The dotted lines are contours at -0.05 and -0.1 .

takes energy from unstable modes near the $k_x=0$ axis to Landau damped modes of nearly the same magnitude near the $k_y=0$ axis. (Realistic simulations of transport therefore require accurate models of Landau damping.) The dissipation near the cutoff indicates a small cascade of fluctuation energy to high k . This picture of energy production in k space is qualitatively similar to that observed in toroidal gyro-fluid simulations. (See Fig. 5.9 of Ref. 6.) The small amount of transfer to high k is dynamically insignificant, so we can conclude that the level of turbulence is set primarily by eddy turnover at long wavelengths. Simulations of just the long wavelengths are therefore theoretically feasible. As we shall see, however, simply eliminating modes that lie beyond the bulk of the spectrum can give catastrophic results as the small transfer of fluctuation energy “piles up” secularly at the cutoff.

IV. EDDY VISCOSITY AND HYPERVISCOSITY

Our model equation can be written symbolically as,

$$\frac{\partial}{\partial \tau} \psi = N(\psi) + L\psi, \quad (18)$$

where L is a linear operator, and N the quadratic nonlinearity defined by Eq. (11). Numerical simulations cannot follow the detailed behavior of the continuous field, ψ . We consider pseudospectral simulations on a periodic box of size $l \times l$, with a finite number of modes. The resolved modes (those that are evolved in a simulation) can be defined through a filter function, $f \rightarrow \bar{f}$, such that, in Fourier space

$$\bar{f}_{\mathbf{k}} = G_{\mathbf{k}} f_{\mathbf{k}}, \quad (19)$$

where $G_{\mathbf{k}} = 1$ for $|k_x| < k_x^c$ and $|k_y| < k_y^c$, and $G_{\mathbf{k}} = 0$ otherwise. (The boundary wavenumbers, k_x^c and k_y^c , are called the cutoff wavenumbers. For theoretical studies of isotropic turbulence, a spherical region in k -space, $|\mathbf{k}| \leq k_c$ is typically used.) Fields such as the potential, ψ , can then be decom-

posed into a resolved part, $\bar{\psi}$, and a subgrid contribution, $\psi^s = \psi - \bar{\psi}$. The filtered evolution equation can be written as

$$\frac{\partial}{\partial \tau} \bar{\psi} = \overline{N(\bar{\psi})} + N^s + L\bar{\psi}, \quad (20)$$

where the subgrid contribution to the nonlinear term is defined by,

$$N^s = \overline{N(\psi)} - \overline{N(\bar{\psi})}. \quad (21)$$

Given the resolved field $\bar{\psi}$, pseudospectral evaluation of the nonlinear term gives precisely $\overline{N(\bar{\psi})}$, so the only term in the evolution Eq. (20) that is not calculated in a simulation of the resolved field is the subgrid contribution, N^s .

The field of Large Eddy Simulation is concerned with deriving approximate models for the effect of the subgrid term, N^s , that can be expressed in terms of the resolved field, $\bar{\psi}$. Traditionally it is argued that the average contribution of the subgrid term, N^s , can be viewed as an eddy viscosity, draining energy from the resolved scales.

If there were a true separation of scales, and the subgrid field ψ^s had asymptotically short wavelengths and short time scales compared to the resolved field $\bar{\psi}$ then the subgrid term would truly act like a viscosity.²⁶ Averaging over a time that is short for the resolved modes but long compared to the turnover time for the subgrid modes, we would find that $\langle N^s \rangle = \nu_{\text{eddy}} \nabla^2 \bar{\psi}$, where the eddy viscosity, ν_{eddy} , is a function of the statistics of the small scales. In reality, however, the length and time scales of the subgrid modes are nearly identical to those of barely resolved modes.

Various approaches to estimating the subgrid contribution have been proposed. We will examine two simple estimates, a k -space dependent eddy viscosity, and the Smagorinsky eddy viscosity.³ In numerical simulations, application of these approaches corresponds to introducing a simple dissipative term [$N_{\mathbf{k}}^s \approx \nu_{\mathbf{k}} k^2 \psi_{\mathbf{k}}$ or $N^s \approx \nabla \nu(\mathbf{x}) \nabla \psi$, respectively] where the damping [$\nu_{\mathbf{k}}$ or $\nu(\mathbf{x})$] is predicted either theoretically or empirically as a function of the resolved scales. Several authors have pointed out that in a turbulent state, subgrid scales do not act in a purely dissipative fashion, and that a more complete model would contain terms to simulate noise and backscatter of energy from the subgrid scales.²⁷ Simple damping terms, however, are extremely efficient to calculate. It is not clear which approach, adding higher order terms to the subgrid model or increasing grid resolution with a simple subgrid model, is more efficient at improving the statistics of the long wavelength modes for a given increase in computational complexity. For the current study, we consider simple dissipative terms.

A. Smagorinsky eddy viscosity

A traditional view of eddy viscosity is that the short wavelength modes in some sense act like a thermal noise on the resolved scales and hence serve to enhance the regular viscosity. Estimating the subgrid contribution by a spatially varying eddy viscosity yields,

$$N^s \approx \nabla \nu_{\text{eddy}}(\mathbf{x}) \nabla \psi(\mathbf{x}). \quad (22)$$

Smagorinsky gave heuristic arguments for the scaling of this eddy viscosity in the context of simulations of quasi-geostrophic turbulence,³ and concluded that,

$$\nu_{\text{eddy}}(\mathbf{x}) = (C_s d)^2 S(\mathbf{x}, t), \quad (23)$$

where C_s is a non-dimensional constant, d is an estimate of the subgrid length scale, and $S(\mathbf{x}, t)$ is the local strain rate of the velocity field defined by,

$$S(\mathbf{x}, t) = \sqrt{\left(\frac{\partial V_x}{\partial x}\right)^2 + \left(\frac{\partial V_y}{\partial y}\right)^2 + \frac{1}{2}\left(\frac{\partial V_x}{\partial y} + \frac{\partial V_y}{\partial x}\right)^2}. \quad (24)$$

Note that $S=0$ for rigid rotation, as well as for uniform flows.

The Smagorinsky model has been applied in computations of flows far outside the realm of its original derivation with success in many cases. This model was used in simulations in this study for the purpose of comparison, to illustrate the behavior of the standard eddy viscosity with k^2 damping. Different choices of length scale and constant have been found to give optimal results in different situations in fluid turbulence. We therefore arbitrarily set d to the physical space grid spacing, and used $C_s=0.1$ based on initial tests for one choice of parameters with moderate resolution.

B. Kraichnan's eddy viscosity

One approach to defining a damping term originating from the subgrid modes is by comparing the nonlinear transfer term with the viscous term in a two-point closure theory.⁴ Considering the splitting of modes into resolved and subgrid, our evolution equation for the quadratic invariant, Eq. (16), can be written as,

$$\left(\frac{\partial}{\partial \tau} - 2\gamma_{\mathbf{k}}\right)\Omega_{\mathbf{k}} = T_{\mathbf{k}}^r + T_{\mathbf{k}}^s, \quad (25)$$

where the transfer defined in Eq. (17) has been decomposed into a resolved piece, $T_{\mathbf{k}}^r$, and the subgrid piece, $T_{\mathbf{k}}^s$. In the context of this equation, the analog to Kraichnan's *effective viscosity* would be defined as,

$$\nu_{\text{eddy}}(\mathbf{k}) = \frac{-\langle T_{\mathbf{k}}^s \rangle}{2k^2 \langle \Omega_{\mathbf{k}} \rangle}, \quad (26)$$

for some appropriately defined ensemble average. The motivation for this definition of an eddy viscosity comes from introducing a damping term of the form, $-\nu_{\text{eddy}}(\mathbf{k})k^2\psi_{\mathbf{k}}$ on the right hand side of the primitive Eq. (10). This damping term would introduce the term $-\langle T_{\mathbf{k}}^s \rangle \Omega_{\mathbf{k}} / \langle \Omega_{\mathbf{k}} \rangle$ to the right hand side of Eq. (25) above, which, on average, will balance the subgrid transfer term, $T_{\mathbf{k}}^s$.

Kraichnan derives predictions of this eddy viscosity⁴ in 2D and 3D Navier-Stokes inertial ranges using the Test Field Model.²⁸ While plasma turbulence is not expected to exhibit inertial range behavior, there are several generic conclusions about eddy viscosity worth noting. The primary discovery was that the eddy viscosity does not give a damping rate proportional to k^2 that is traditionally associated with an eddy viscosity. The eddy viscosity does asymptote to a constant value at long wavelengths. This constant, however, is negative for 2D turbulence. The major contribution to the

subgrid energy transfer comes from coherent straining of the short wavelength modes by long wavelength velocity shear, which causes the eddy viscosity to become large and positive near the high-wavenumber cutoff, k_c . Our simulations correspond most closely to the two-dimensional case where the cutoff, k_c , lies in the enstrophy range. For this case, the significant positive contribution to the eddy viscosity lies in a region near the cutoff wavenumber, k_c , of width k_0 , where the straining field is dominated by wavenumbers of size k_0 and smaller. The shape of the eddy viscosity function in this region depends on the nature of the spectrum at long wavelengths. For an artificial spectrum that allowed for a simpler calculation, the eddy viscosity in the near cutoff region was found to be

$$\nu_{\text{eddy}}(k) \approx (\theta k_c k_0)^{-1} f\left(\frac{k_c - k}{k_0}\right), \quad \text{for } (k_c - k) \ll k_c, \quad (27)$$

where θ is eddy circulation time of the long wavelengths. [See Eq. (6.5) in Ref. 4.]

C. Numerical eddy viscosity

In the original work on this eddy viscosity,⁴ the subgrid transfer, $\langle T^s \rangle$, was viewed as a theoretically derived quantity containing contributions from all three-mode couplings that cross the cutoff in k -space. The standard approach to calculating eddy viscosity in numerical simulations^{29,30} defines the subgrid transfer based on the subgrid contribution to the nonlinear term as defined in Eq. (21). For our model the subgrid transfer is defined by,

$$T_{\mathbf{k}}^s = [(1 + |\mathbf{k}|^2)^2 + \delta_0^2 k_y^2] (\psi_{\mathbf{k}} N_{\mathbf{k}}^{s*} + \psi_{\mathbf{k}}^* N_{\mathbf{k}}^s). \quad (28)$$

Substituting this definition for T^s into the definition of eddy viscosity in Eq. (26), we find that

$$\nu_{\text{eddy}}(\mathbf{k}) = -\frac{\text{Real}(\langle \psi_{\mathbf{k}}^* N_{\mathbf{k}}^s \rangle)}{k^2 \langle |\psi_{\mathbf{k}}|^2 \rangle}. \quad (29)$$

Using this definition, the eddy viscosity approximation for the subgrid term,

$$N_{\mathbf{k}}^s \approx -\nu_{\text{eddy}}(\mathbf{k})k^2\psi_{\mathbf{k}}, \quad (30)$$

can be viewed as the linear (in $\psi_{\mathbf{k}}$) approximation that minimizes the mean squared residual error.

To calculate the eddy viscosity for a given low resolution simulation with cutoff wavenumber k_c , a simulation is performed at much higher resolution containing a large number of higher k modes ($|k| > k_c$) along with all the modes resolved by the low resolution simulation. The "unresolved" component of the nonlinear term, N^s , defined in Eq. (21), is calculated for the low resolution simulation from modes resolved in the higher resolution simulation. Calculating the eddy viscosity from high resolution simulations to apply to low resolution simulations cannot by itself reduce the computational cost of a particular problem since presumably the high resolution simulations yield accurate results already. It is hoped that by parameterizing the eddy viscosity calculated for a number of runs, we can obtain a model for the eddy viscosity that extrapolates to drift wave problems for a larger range of parameters.

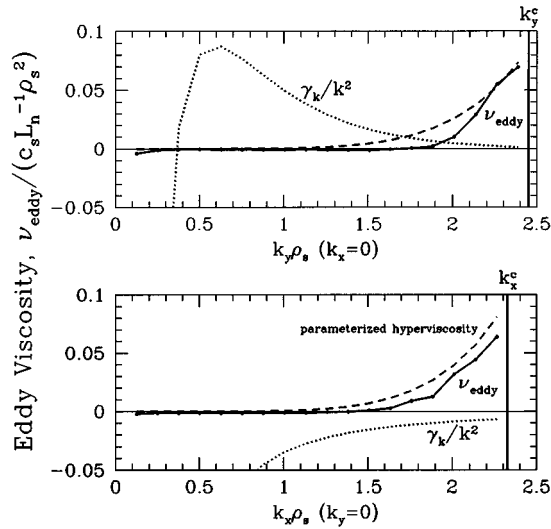


FIG. 6. Eddy viscosity calculated for the simulation of Fig. 2. The transfer was calculated for a box of 37×39 modes (representing a simulation with half the actual resolution) to modes outside the box, but resolved by the simulation. The dotted line is the linear growth rate, expressed as a viscosity by dividing by k^2 . The eddy viscosity has a small negative component as $k \rightarrow 0$, but it is negligible compared to the linear driving term. The eddy viscosity becomes important in a small region near the cutoff. The dashed line is the parameterized hyperviscosity derived in Sec. V. For these parameters and cutoff wavenumber the parameterization provides a good fit to the actual eddy viscosity.

The sample simulation mentioned in Sec. III was used to calculate the eddy viscosity for a simulation with half of its resolution. The resulting eddy viscosity $v_{\text{eddy}}(\mathbf{k})$ is plotted in Fig. 6 with the linear drive and damping for lines of modes out to the cutoff wavenumber in two directions in k -space. As noted in Sec. III, we do not expect inertial range behavior in simulations of this kind of plasma turbulence, and there is no inverse cascade of energy from very short wavelengths. While there is a small negative eddy viscosity at long wavelengths for this simulation, it is dynamically insignificant compared to the linear drive and dissipation at long wavelengths. The dominant effect of the eddy viscosity lies in a narrow region near the cutoff where it becomes positive and large compared to the linear drive. The mechanism for this damping near the cutoff is the loss of fluctuation energy from resolved modes by the coherent straining due to long wavelength modes.⁴ This damping mechanism is probably the dominant physical effect of subgrid modes in drift wave turbulence simulations, so the focus of this study is to effectively model the positive eddy viscosity in the region near the cutoff.

D. Heuristic arguments for the scaling of the eddy damping rate

Consider a fictitious wave packet of short wavelength fluctuations, localized in k -space and real space so that the long wavelength advecting velocity field looks locally like a shear flow. Without loss of generality, consider the action of the local shear flow, $\mathbf{v}_E(x, y) = -\theta^{-1} y \hat{\mathbf{x}}$, where the shearing

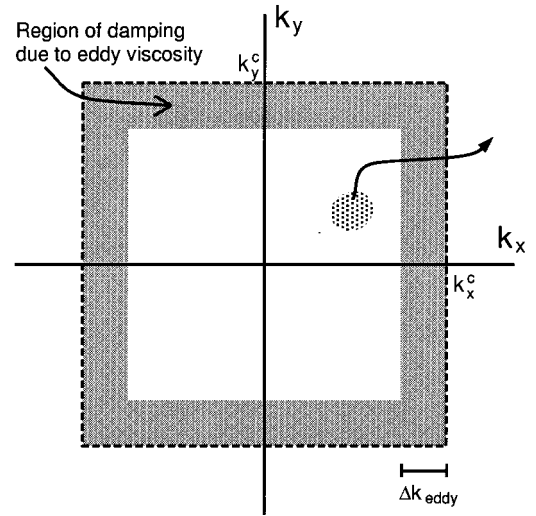


FIG. 7. Heuristic picture of a fluctuation wave packet undergoing shear. As discussed in Sec. IV D, the region of significant eddy viscosity near the cutoff (the grey region), acts as an absorbing buffer for fluctuation energy that would leave the system unaided if the system were truly unbounded.

time is denoted by θ . The advection part of the continuity equation then has the form of a shear flow in Fourier space as well,

$$\frac{\partial}{\partial t} \tilde{n}_i(\mathbf{k}) + \theta^{-1} \frac{\partial}{\partial k_y} k_x \tilde{n}_i(\mathbf{k}). \quad (31)$$

Figure 7 illustrates this process. The wave packet will be advected in k -space in a particular direction depending on the local shear. The random variations of the local shear will thus lead to a random walk diffusion of this wave packet in k -space, with a net transfer of fluctuation energy to high k .³¹

In the numerical simulation, however, the absence of the nonlinear interactions with unresolved modes and the conservative nature of the nonlinearity cause the cutoff in k -space to act as a reflecting boundary. Thus in Fig. 7, the wave packet, represented by the dark circle, would be reflected back to long wavelengths instead of leaving the system. A reasonable estimate of the amount of eddy damping required by an eddy viscosity, therefore, would be given by the inverse of the time which a wave packet spends in the near cutoff region of width Δk_{eddy} where the eddy viscosity operates. (In reality a wave packet may enter and leave this region of k -space several times as it random walks to the dissipation range. Thus we do not expect the actual eddy viscosity needs to be large enough to fully damp fluctuations before they are reflected back to large scales.) For this example, the velocity of the packet in k -space is $\theta^{-1} k_x$ so the time it spends in the edge region is $\theta k_x^{-1} \Delta k_{\text{eddy}}$. An eddy damping rate of the form,

$$\gamma_{\text{eddy}}(k) \sim -\theta^{-1} k_c \Delta k_{\text{eddy}}^{-1} f \left[\frac{k_c - k}{\Delta k_{\text{eddy}}} \right], \quad (32)$$

would therefore effectively damp fluctuations being sheared to high wavenumber. The maximum damping rate given by the theoretical enstrophy range eddy viscosity defined in Eq.

(27) scales as $\nu_{\text{eddy}}(k_c)k_c^2 \approx \theta^{-1}k_c k_0^{-1}$ while $-\gamma_{\text{eddy}}(k_c) \times k_c^2 \sim \theta^{-1}k_c \Delta k_{\text{eddy}}^{-1}$, so the same basic scaling is obtained if we identify k_0 with Δk_{eddy} .

E. Hyperviscosity

Hyperviscosity is defined as a damping term of the form

$$\gamma_{\mathbf{k}}^d = -\nu_h \left(\frac{|\mathbf{k}|}{k_c} \right)^p, \quad (33)$$

where p is larger than two. Hyperviscosity has been used for a long time as a numerical tool for simulating high Reynolds number turbulence, in order to provide an artificial dissipation range in the resolved modes. Hyperviscosity has been regarded as an artificial damping term that does not attempt to estimate the subgrid interaction. Authors have, however, viewed hyperviscosity as a kind of subgrid model in the way that it serves as a sink for small scale fluctuation energy.²

The choice of power p and size of the hyperviscosity ν_h is rarely discussed in the literature. Typically the size of the damping is set experimentally so that a dissipation range appears within the resolved modes. Studies of 2D Navier-Stokes turbulence² have found that large powers ($p \sim 16$) work well, but that the optimal choice depends on the resolution of the simulation. With insufficient damping at the cutoff fluctuation energy will tend towards equipartition in the Fourier modes leading to a spectrum $\Omega(k) \propto k$ towards the cutoff which disagrees with the converged dissipative result. If the power used is too small, then damping that is sufficient to prevent unphysical behavior at the cutoff will introduce significant damping at long wavelengths and strongly affect the results. On the other hand, there must clearly be an upper limit to the power used. For a very high power there would be virtually no damping for almost all the modes except for a few modes near the cutoff which would be extremely damped. The results would be similar to performing a simulation with those modes removed and no damping on the remaining modes. This behavior may be considered analogous to impedance matching at the end of an electrical cable, where strong reflections occur if the load impedance is either too small or too large.

The constant, ν_h , is typically chosen so that modes near the cutoff experience damping that is large compared to the eddy turnover rate. An artificial dissipation region is introduced into the resolved modes that is much narrower in k -space than the dissipation region given by the usual k^2 damping term. If the precise form of the dissipation does not affect the large scale dynamics (as we will find in Sec. VI), then the use of artificial damping terms like hyperviscosity can yield significant savings in computation by greatly reducing the required resolution.

V. HYPERVISCOSITY AS A MODEL FOR EDDY VISCOSITY

The exact form of the eddy damping depends on the detailed nature of the saturated spectrum and the mode-mode coupling to unresolved modes. If one could accurately predict the eddy viscosity from theory then there would be no point in performing numerical simulations. There are a large

number of models for drift wave turbulence each of which will saturate with a different spectrum, so in general we will expect a different eddy viscosity from that predicted for Navier-Stokes turbulence by Kraichnan.⁴ Hence we are motivated to parameterize the basic features of the eddy viscosity in terms of the large scale flow.

Hyperviscosity provides significant damping in a narrow region near the cutoff wavenumber, just as the calculated eddy damping for this model does (Fig. 6). An obvious method of fixing the two hyperviscosity parameters, the power p and magnitude M in Eq. (36), is to match the width and overall damping rate with the calculated eddy damping term. The width and the damping are functions of the large scale flow, so to apply the results to simulations we must define quantities corresponding to the long wavelength scale k_0 and eddy circulation time θ . As a surrogate for the long wavelength eddy turnover time we used the volume averaged shearing rate,

$$S(t) = \left(\frac{1}{A} \int S(\mathbf{x}, t)^2 d\mathbf{x} \right)^{1/2}. \quad (34)$$

An average wavenumber of the large scales is given by dividing the rate of shear by the root mean square of the velocity field,

$$k_{\text{av}} = S \left(\frac{1}{A} \int V_x^2 + V_y^2 d\mathbf{x} \right)^{-1/2}. \quad (35)$$

We will use the average wavenumber k_{av} as an estimate for the long wavelength scale k_0 and the inverse rate of shear $S(t)^{-1}$ as an estimate for the eddy circulation time θ .

The hyperviscosity used for the simulations considered here introduces a damping term of the form,

$$\gamma_h = -M \left[\left(\frac{k_x}{k_{xc}} \right)^p + \left(\frac{k_y}{k_{yc}} \right)^p \right], \quad (36)$$

into the model, Eq. (10), by setting $\gamma_{\mathbf{k}}^d = \gamma_h$. This hyperviscous damping term, γ_h , can be compared to the damping rate, $\nu_{\text{eddy}}(\mathbf{k})k^2$, given by the theoretical eddy viscosity of Eq. (27), and to the heuristic eddy damping rate defined in Eq. (32). The width of the theoretical eddy viscosity scales with the long wavelength scale k_0 while the width of this hyperviscosity scales as k_c/p , so we expect to find that $p \propto k_c/k_{\text{av}}$. Comparing the magnitude of the three damping rates at the cutoff wavenumber k_c , we expect the magnitude to scale as $M \propto S k_c/k_{\text{av}}$.

An estimate for the power p and magnitude M was obtained from the numerically calculated eddy viscosity by setting two moments in k -space to zero,

$$\sum_{\mathbf{k}} (-\nu_{\text{eddy}}(\mathbf{k})k^2 - \gamma_h) = 0, \quad (37)$$

$$\sum_{\mathbf{k}} (-\nu_{\text{eddy}}(\mathbf{k})k^2 - \gamma_h) \min(k_{xc} - |k_x|, k_{yc} - |k_y|) = 0.$$

This estimate matches the width and magnitude of the damping region given by the hyperviscosity to that of the eddy viscosity. The estimate for the power and magnitude from simulations with a range of parameters and resolutions are

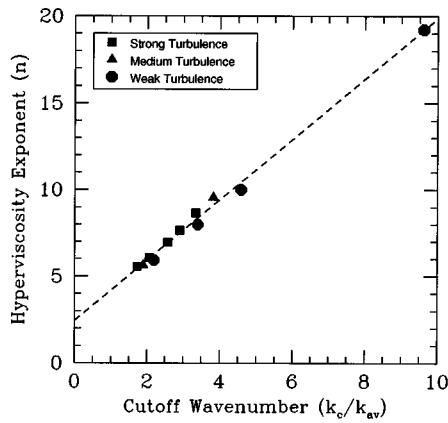


FIG. 8. Hyperviscosity power predicted from direct numerical simulations.

summarized in Figs. 8 and 9. The scaling of the power (and hence the width of the damping region), seems very robust. The estimate from these simulations gives

$$p \sim 1.7k_c/k_{av} + 2.4, \quad (38)$$

$$M \sim 0.1Sk_c/k_{av}.$$

The scaling of the magnitude (Fig. 9) is less robust than the scaling of the power (Fig. 8). There may be other macroscopic quantities that can be used to refine the estimate for the size of the damping.

VI. TESTS OF HYPERVISCOSITY

Simulations were performed for a range of parameters, and grid sizes ranging from 32×32 to 256×256 to test the performance of three dissipation models against each other and against the use of no dissipation model. An ordinary hyperviscosity was tested with power $p = 16$ and coefficient set based on the rate of shear, $\nu_h = S$. The Smagorinsky eddy viscosity was tested with the constant $C_s = 0.1$ chosen arbitrarily. Based on the results from the previous section, we tested the parameterized hyperviscosity with power $p = 1.7k_c/k_{av} + 2.4$ and magnitude $M = 0.1S(t)k_c/k_{av}$.

Typically simulations of isotropic turbulence will use an *a priori* fixed power hyperviscosity to provide the necessary

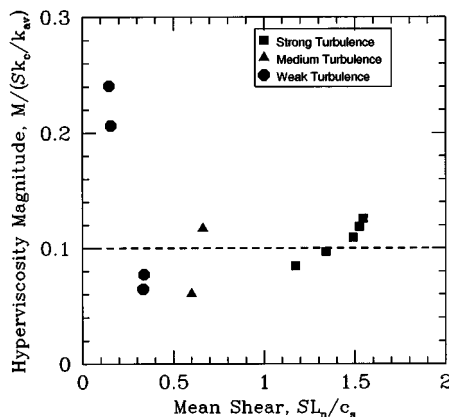


FIG. 9. Hyperviscosity magnitude predicted from direct numerical simulation.

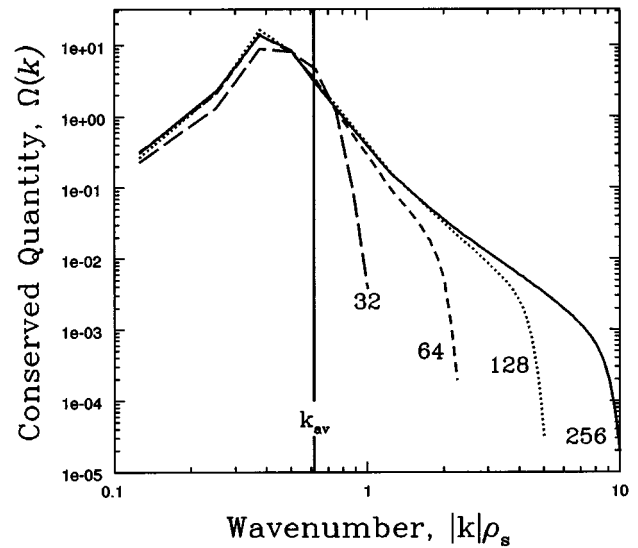


FIG. 10. Convergence of simulations using hyperviscosity at moderate turbulence levels. (The parameters, $\delta_0 = 0.15$, $\alpha = 0.015$, and $\mu = 0.0001$, were used with periodic box size $50\rho_s \times 50\rho_s$.) A hyperviscosity with an *a priori* fixed power $p = 16$ was used as is typically done in simulations of isotropic turbulence. The damping was set to the rate of shear ($\nu_h = S$) to ensure that resolved high- k modes were sufficiently damped. The large scale average wavenumber, k_{av} , calculated from the highest resolution simulation is included for reference.

damping. Resulting spectra for simulations using the fixed power hyperviscosity are shown in Fig. 10 for the parameter choice that gave moderate levels of turbulence. We expect the rate of transfer of fluctuations to short wavelengths to scale with the rate of shear S , so our choice of a hyperviscous damping of the form $S(k/k_c)^p$ corresponds to setting the dissipation wavenumber to a fixed fraction of the cutoff wavenumber k_c . (The dissipation wavenumber is the scale at which the damping of the conserved quantity becomes dynamically significant.) The spectrum at long wavelengths observed in simulations²⁴ is a slowly changing function of Reynolds number for the 2D Navier-Stokes enstrophy cascade where hyperviscosity is the primary source of dissipation. Since the physics of our drift-wave model is dominated by production and dissipation of fluctuations at long wavelengths (see Fig. 5), we expect to find an even weaker dependence of the long wavelength saturation on the precise details of the dissipation range. Moving the hyperviscous dissipation scale with the cutoff allows us to resolve more of the small scale dynamics with increased resolution. The spectra are almost identical at long wavelengths for grid sizes 128×128 and 256×256 , so we are confident that the 256×256 case well represents the converged solution.

The results of simulations using no eddy viscosity or hyperviscosity term are shown in Fig. 11 for comparison. It is well known that lack of an eddy viscosity leads to unphysical results in Navier-Stokes turbulence when the small scale dissipation wavenumber exceeds the cutoff. One might think that since dissipation from terms that model Landau damping at long wavelengths is the dominant drain of energy then the transfer to small spatial scales can be completely ignored. From the results, we can see that this hypothesis is

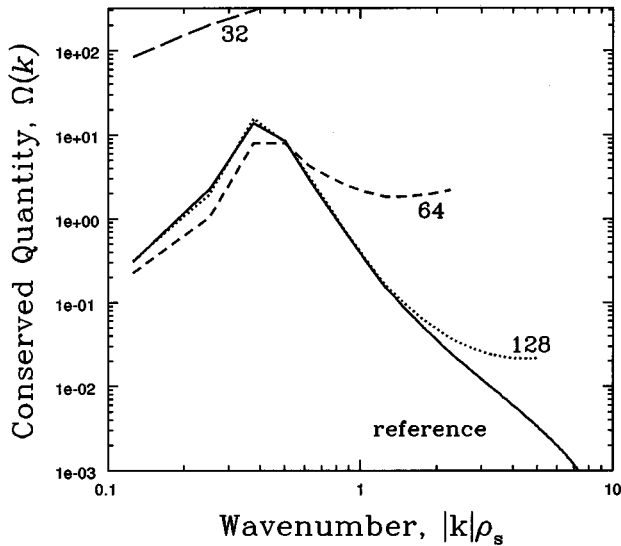


FIG. 11. Convergence of simulations using no added dissipative terms for the same choice of parameters used in Fig. 10. The lower resolution results failed to give reasonable results in this case.

only partially true. Given sufficient resolution, the spectrum converges to the reference spectrum obtained from the highest resolution hyperviscosity run. The lower resolution runs, however, give wildly inaccurate results despite the fact that the lowest resolution considered here (32×32) resolves the primary production and dissipation wavenumbers in Fig. 5. Drift wave turbulence will typically exhibit only a moderate separation of scales between the spectral peak and the dissipative range, so it is practical to perform 2D simulations with sufficient resolution that an eddy viscosity or hyperviscosity term is unnecessary. On the other hand, for three-dimensional simulations of drift wave turbulence, the reduction in required resolution can be significant.

Performance of the Smagorinsky eddy viscosity with constant, $C_s = 0.1$, for the same parameter choice is shown in Fig. 12. Again, given sufficient resolution, the spectrum converges to the reference spectrum. Results at long wavelengths ($k\rho_s \sim 0.4$) for lower resolution runs are better than those obtained using no additional dissipation terms but not as good as those obtained using a hyperviscosity. We found that choosing a larger value of the constant C_s will improve the results somewhat at lower resolution but degrades the results for the 128×128 case. The constant C_s is probably not universal for the kind of turbulence we are studying here, in contrast to the case of the inertial range in Navier-Stokes turbulence. A fundamental problem with applying any eddy viscosity that gives damping scaling as k^2 , however, is that providing sufficient damping for modes near the cutoff forces one to introduce a significant artificial damping into the long wavelength modes that dominate the nonlinear physics.

Simulation results using the parameterized hyperviscosity are shown in Fig. 13. In this case, results at low resolution are obtained that are superior to those from all other approaches considered in our study. The performance of the parameterized hyperviscosity indicates that it provides a rea-

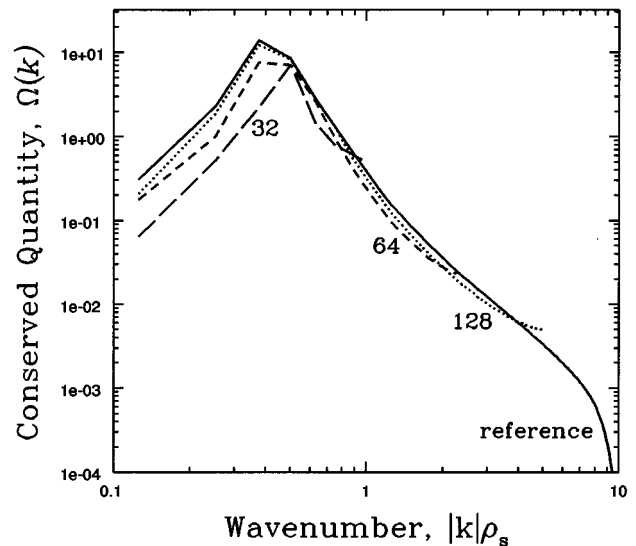


FIG. 12. Convergence of simulations using the Smagorinsky eddy viscosity with $C_s = 0.1$, for the same choice of parameters used in Fig. 10.

sonable model of the actual eddy damping process. Note that in the lowest resolution run here, a significant portion of driven modes lie beyond the cutoff wavenumber, so the spectrum falls below the reference spectrum. It is possible that even better results may be obtained for low resolution simulations by modeling the transfer of energy from unresolved small scales to resolved long wavelengths by adding a negative term to the eddy viscosity to model this backscatter.

Convergence of the measured flux is summarized for simulations of weakly driven, moderately driven, and strongly driven turbulence (Figs. 14, 15, and 16, respectively). In each case, the measured flux is normalized to a reference value obtained from a high resolution (grid size 256×256) simulation using hyperviscosity. In all cases the

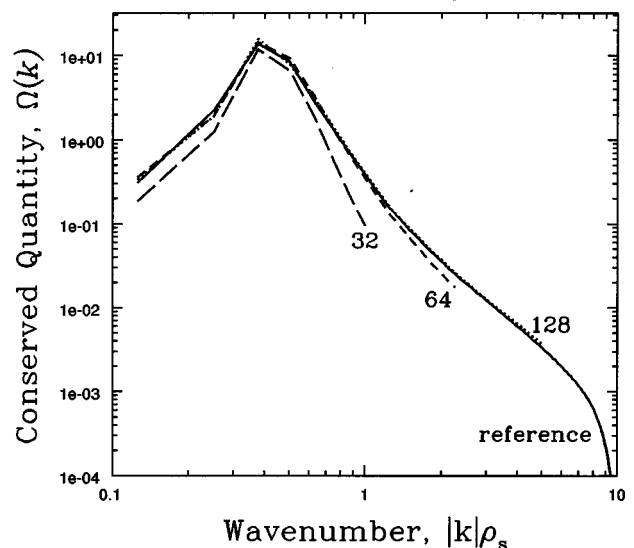


FIG. 13. Convergence of simulations using the parameterized hyperviscosity ($p = 1.7k_c/k_{av} + 2.4$, $M = 0.1Sk_c/k_{av}$) for the same choice of parameters used in Fig. 10.

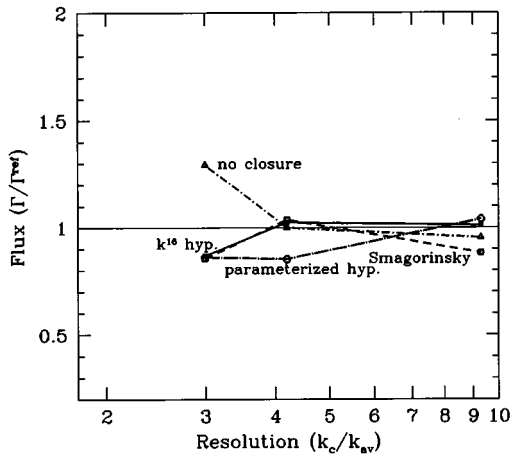


FIG. 14. Convergence of the measured flux as a function of resolution for the case of weakly driven turbulence. (The parameters, $\delta_0=0.20$, $\alpha=0.03$, and $\mu=0.0001$, were used with periodic box size $40\rho_s \times 40\rho_s$.) The flux is normalized to the flux measured by a reference simulation where $k_c/k_{av} \approx 13$. In this case the nonlinear transfer to shorter wavelengths is a small effect, so the use of a subgrid damping term is unnecessary.

most reasonable results obtained at lower resolution were obtained using the parameterized hyperviscosity or the k^{16} hyperviscosity. For the moderate and strong turbulence cases, one obtains reasonable results at resolutions at least a factor of 2 smaller than those necessary for simulations with no added dissipation. For the case of weakly driven turbulence, however, the nonlinear coupling to unresolved modes is less important and there is little difference between any of the models used. In summary, a hyperviscous damping term works effectively in drift wave simulations at low resolutions (working down to $k_c/k_{av} \sim 4$) and moderate to strong levels of turbulence.

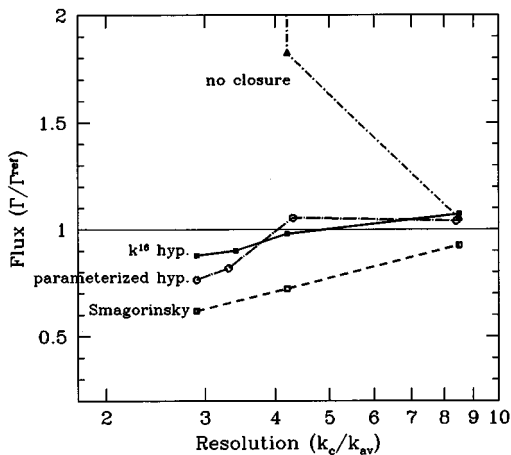


FIG. 15. Convergence of the measured flux as a function of resolution for the cases of moderately driven turbulence. (See Fig. 10 for the parameters.) The flux is normalized to the flux measured by a reference simulation where $k_c/k_{av} \approx 15$. In this case the nonlinear transfer is sufficiently strong that the simulations will blow up with no damping term for lower resolution runs. A high powered hyperviscosity outperforms the Smagorinsky viscosity.

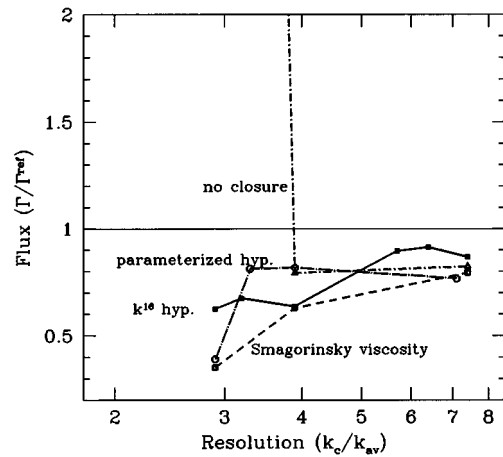


FIG. 16. Convergence of the measured flux as a function of resolution for the cases of strongly driven turbulence. (See Fig. 2 for the parameters.) The flux is normalized to the flux measured by a reference simulation where $k_c/k_{av} \approx 13$. The results are similar to those obtained for the case of moderately driven turbulence (Fig. 15).

VII. RESOLUTION REQUIREMENTS

We have observed that if the cutoff wavenumber is at least a factor of 3 or so greater than the long wavelength scale, k_{av} , (or roughly a factor of 6 larger than the spectral peak wavenumber), then reasonable results can be obtained with the use of a hyperviscosity. There are several sources of error in calculating macroscopic quantities such as the flux from lower resolution simulations. Contributions to the flux from unresolved modes may be significant or the resolved modes may fail to saturate at the correct level. Incorrect saturation levels may be due to the failure of our parameterization to model the eddy viscosity or from the failure of eddy viscosity to model the physics of unresolved modes.

For the lowest resolution simulations considered in this study, the contribution to the flux from unresolved modes, is too small (5% or less) to explain the discrepancy between the calculated flux at low and high resolution. As is clear from the spectra in Figs. 10 and 13, the error in the calculated flux at the lowest resolution comes from the failure of resolved modes to saturate at the correct level. The eddy viscosity calculated for grid size 32×32 for moderate levels of turbulence is plotted in Fig. 17. The parameterization overestimates the eddy viscosity significantly in this case. As well, the calculated eddy viscosity is significantly anisotropic and the negative viscosity at long wavelengths is of comparable size to the positive portion that the parameterization models. For comparison, we used the calculated eddy viscosity in a simulation at this resolution. The resulting spectrum is shown compared to the hyperviscosity simulations and the high resolution reference spectrum in Fig. 18. Using the calculated eddy viscosity gives very accurate results in this case. The flux calculated from this simulation is within 5% of the flux calculated from the highest resolution run.

The current limits of the parameterized hyperviscosity are therefore clearly due to its failure to model accurately the eddy viscosity at low resolution. Future work will attempt to improve the parameterization of the magnitude of the hyper-

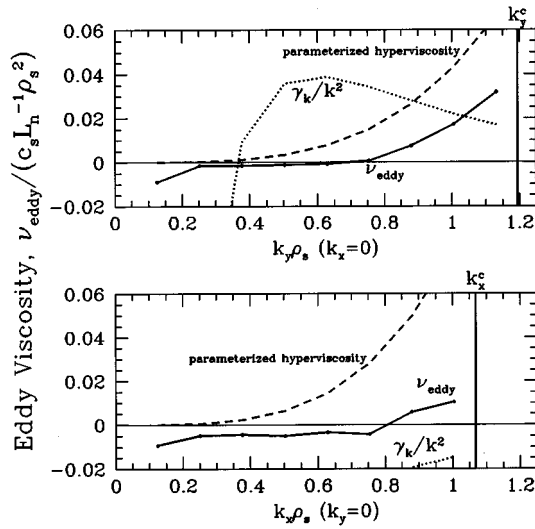


FIG. 17. Eddy viscosity calculated for a low resolution simulation at moderate levels of turbulence. (See Fig. 10 for the parameters.) In this case, the parameterized hyperviscosity grossly overestimates the damping. Note that the calculated eddy viscosity is anisotropic in this case and has a significant negative component at long wavelengths. Simulations at this resolution estimated $k_c/k_{\text{av}} \approx 3$.

viscosity, generalize the parameterization to provide anisotropic damping, and possibly to incorporate a model for the negative viscosity at long wavelengths. It is not clear from this work which of these improvements will have the greatest effect on improving the accuracy of low resolution simulations.

VIII. CONCLUSIONS

A new parameterized hyperviscosity, Eqs. (36) and (38), was derived by analyzing the eddy viscosity calculated from simulations with a range of parameters and resolutions. Simulations using the parameterized hyperviscosity perform somewhat better than those using hyperviscosity with fixed power, and significantly better than those using no extra

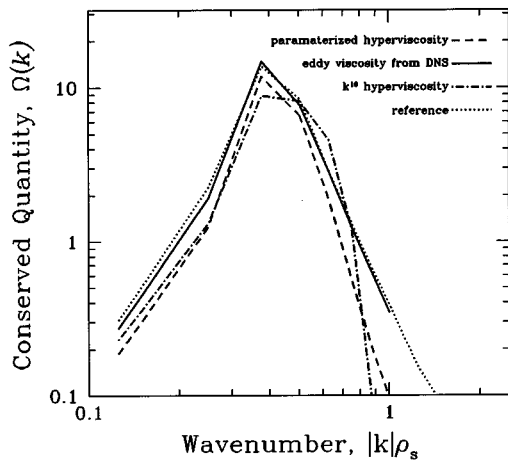


FIG. 18. Comparison of simulations at low resolution using hyperviscosity and the calculated eddy viscosity in Fig. 17. (At this resolution, the Smagorinsky eddy viscosity gives very poor results, and simulations with no added dissipative term blow up.)

damping term, or a Smagorinsky-type eddy viscosity. Accurate results are obtained provided the cutoff wavenumber, k_c , is approximately four or more times greater than the characteristic wavenumber of the advecting velocity, k_{av} . At lower resolutions, the parameterization fails to accurately model the eddy viscosity.

This new hyperviscosity model is easy to implement in 3D pseudospectral simulations. Finite difference analogues involving ∇^p operators are conceivable, but would require more effort to implement, and generalizations to non-uniform turbulence with boundary layers would be a topic for another study.

Because this hyperviscosity is based on physics generic to most drift-wave turbulence, application to more complete models is straightforward. This hyperviscosity is very useful computationally, since reducing resolution requirements by even a factor of 2 reduces the computational requirements by a factor of 8 in two dimensions, or 16 in three dimensions.

ACKNOWLEDGMENTS

Dr. A. Chekhlov graciously provided a 2D Navier-Stokes pseudospectral code that was modified for use in this study. We would like to thank Professor S. A. Orszag for his guidance in initiating this research and for his feedback. Several useful discussions were had with Dr. J. Krommes. Most of the computations were carried out on a Cray YMP at the National Energy Research Supercomputer Center, Lawrence Livermore National Laboratory.

This work was supported by U. S. Department of Energy Contract Nos. DE-AC02-76CH03073 and DE-FG02-93ER54204, and by a graduate fellowship from the Natural Sciences and Engineering Research Council of Canada.

- ¹Large Eddy Simulation of Complex Engineering and Geophysical Flows, edited by B. Galperin and S. A. Orszag (Cambridge University Press, Cambridge, 1993).
- ²C. Basdevant and R. Sadourny, J. Méc. Théor. Appl., Numéro Spécial, 243 (1983).
- ³J. Smagorinsky, Mon. Weather Rev. **91**, 99 (1963).
- ⁴R. Kraichnan, J. Atmos. Sci. **33**, 1521 (1976).
- ⁵A. Chekhlov, Ph.D. thesis, Princeton University, 1995.
- ⁶M. Beer, Ph.D. thesis, Princeton University, 1994.
- ⁷G. Hammett and F. Perkins, Phys. Rev. Lett. **64**, 3019 (1990).
- ⁸W. Dorland, Ph.D. thesis, Princeton University, 1993.
- ⁹G. W. Hammett, M. A. Beer, W. Dorland, S. C. Cowley, and S. A. Smith, Plasma Phys. Controlled Fusion **35**, 973 (1993).
- ¹⁰A. M. Dimits, J. A. Byers, T. J. Williams, B. I. Cohen, X. Q. Xu, R. H. Cohen, J. A. Crotinger, and A. E. Shestakov, in *Plasma Physics and Controlled Nuclear Fusion Research, 1994* (International Atomic Energy Agency, Vienna, 1994), Vol. 2, pp. 457–462.
- ¹¹R. E. Waltz, G. D. Kerbel, and J. Milovich, Phys. Plasmas **1**, 2229 (1994).
- ¹²A. Hasegawa and K. Mima, Phys. Fluids **21**, 87 (1978).
- ¹³P. Terry and W. Horton, Phys. Fluids **25**, 491 (1982).
- ¹⁴Y.-M. Liang, P. Diamond, X.-H. Wang, D. Newman, and P. Terry, Phys. Fluids B **5**, 1128 (1993).
- ¹⁵W. W. Lee, Phys. Fluids **26**, 556 (1983).
- ¹⁶D. H. E. Dubin, J. A. Krommes, C. Oberman, and W. W. Lee, Phys. Fluids **26**, 3524 (1983).
- ¹⁷W. W. Lee, J. Comput. Phys. **72**, 243 (1987).
- ¹⁸W. Dorland and G. W. Hammett, Phys. Fluids B **5**, 812 (1993).
- ¹⁹R. E. Waltz, R. R. Dominguez, and G. W. Hammett, Phys. Fluids B **4**, 3138 (1992).
- ²⁰M. A. Beer, S. C. Cowley, and G. W. Hammett, Phys. Plasmas **2**, 2687 (1995).

- ²¹A. M. Dimits, T. J. Williams, J. A. Byers, and B. I. Cohen, Phys. Rev. Lett. **77**, 71 (1996).
- ²²R. H. Kraichnan, Phys. Fluids **10**, 1417 (1967).
- ²³G. K. Batchelor, Phys. Fluids Suppl. **II**, 233 (1969).
- ²⁴V. Borue, Phys. Rev. Lett. **71**, 3967 (1993).
- ²⁵P. Diamond and H. Biglari, Phys. Rev. Lett. **65**, 2865 (1990).
- ²⁶R. Kraichnan, Complex Syst. **1**, 805 (1987).
- ²⁷H. Rose, J. Fluid Mech. **81**, 719 (1977).
- ²⁸R. H. Kraichnan, J. Fluid Mech. **47**, 513 (1971).
- ²⁹M. E. Maltrud and G. K. Vallis, Phys. Fluids A **5**, 1760 (1993).
- ³⁰A. Chekhlov, S. Orszag, S. Sukoriansky, B. Galperin, and I. Staroselsky, Phys. Fluids **6**, 2548 (1994).
- ³¹C. E. Leith, Phys. Fluids **11**, 671 (1968).